



Comparative analysis of fouling mechanisms of ceramic and polymeric micro-filtration membrane for algae harvesting

Pooreum Kim^a, Kitae Park^a, Hyoung Gun Kim^b, JiHoon Kim^{a,*}

^aGraduate School of Water Resources, Sungkyunkwan University, Suwon, Korea, Tel. +82-31-290-7647;
Fax: +82-31-290-7549; email: jjtt23@skku.edu (J.H. Kim)

^bPOSCO E&C tower, 241, Incheon tower-daero, Yeonsu-gu, Incheon, Korea

Received 21 January 2019; Accepted 30 June 2019

ABSTRACT

This study aims to derive operating properties by membrane material in membrane processes applied to maintain the concentrations of algae harvesting using artificial feed water replicating algae raw water and then to analyze the fouling formation mechanisms. This study selected two types of membranes: polyvinylidene fluoride polymeric membrane representing hydrophobicity and silicon carbide ceramic membrane representing hydrophilicity. Existing Hermia's model was used to analyze the fouling formation mechanisms when inpouring algae. When filtering polymeric and ceramic membranes in high concentrations of artificial algae raw water, it was able to operate ceramic membranes with much higher LMH (L/m² h). It was confirmed that fouling occurs less frequently due to ceramic membranes' properties such as hydrophilicity and highly negative charge. Hermia's model was used to examine the membrane fouling mechanisms. Both results showed different fouling formation mechanisms. It is considered that this was caused by the hydrophilicity of the polymeric membranes and the relative hydrophobicity of the ceramic membranes. It was confirmed that the fouling tendency varied from membrane materials. Membrane materials are regarded as a major reason. Results, examining the fouling formation mechanisms using Hermia's model is considered as an important factor in fouling control when applying membrane processes from the perspective of algae harvesting.

Keywords: Ceramic membrane; Algae harvesting; Fouling; Algal bloom; Hermia's model; Microfiltration membrane

1. Introduction

Recently, extreme weather and environmental pollution have had a tremendous effect on water resources, and it is estimated environmental pollution will be worse. In particular, the occurrence of algal blooms by algae every summer in rivers and lakes has grown anxiety of drinking water. It is reported that these algae negatively affect water purification processes by disturbing water systems degrading water quality and increasing turbidity [1]. Although membrane processes widely used in water treatment fields in recent years have been reported that they remove algal

substances mentioned above [2], it is clear that algae are serious fouling factors. According to previous studies, algae harm membranes and affect fouling properties [3]. In particular, it has been reported that algae form biofilms and increase membrane fouling by biofouling and extracellular polymeric substances (EPS) such proteins and polysaccharides primarily cause membrane fouling [4]. Effective processes for algae removal include a method for combining coagulation and precipitation processes using low-pressure membranes [5]. Removal processes such as ultrasonic pretreatment for algae removal have been continuously developed [6]. Particularly,

* Corresponding author.

it has been reported that the method for combining coagulation and precipitation processes improves algae removal [7]. However, because treatment is difficult when high concentrations of algae are flown and there are limitations to treatment using single membrane process, active studies have been conducted to use processes with other pretreatment processes [8]. Moreover, it has been recognized that existing polymeric membranes should be widely used in water treatment processes for effective algae removal [9], but water treatment using ceramic membranes has been recently studied because of advantages such as higher chemical safety and better hydrophilicity than existing polymeric membranes [10].

This study aims to derive operating properties by membrane material in membrane processes applied to maintain the concentrations of algae harvesting using artificial feed water replicating algae raw water and then to analyze the fouling formation mechanisms. This study selected two types of membranes: polyvinylidene fluoride (PVDF) polymeric membrane representing hydrophobicity and silicon carbide ceramic membrane representing hydrophilicity. Existing Hermia's model was used to analyze the fouling formation mechanisms when inpouring algae.

2. Materials and methods

2.1. Feed water properties

Chlorella-based artificial algae were used as feed water at a suitable concentration in this study. Table 1 shows the detailed analysis results of artificial feed water used in the experiments.

2.2. Membranes

Two types of membranes (polymeric and ceramic membranes) were used in the experiments. The polymeric membrane has the form of hollow fibers and is made of PVDF commercialized by Company A, and the ceramic membrane is a flat type MF membrane manufactured by Cembrane (Denmark). Both of the modules were refrigerated by immersing in a 1% sodium hypochlorite (NaOCl) solution. The specifications of the used membranes are as shown in Table 2.

2.3. Test unit

A lab-scale experimental device connecting hollow fiber formed and flat type polymeric membranes were used in this

experiment. As shown in Fig. 1, this device consists of a 100 L feed water tank, 20 L treatment tank for backwashing (B/W), a metering pump (EMS-2000S, South Korea), a stirrer, a flow meter, and a digital pressure gauge to realize automatic and continuous operation. The digital pressure gauge was connected to the laptop so that it was able to monitor transmembrane pressure (TMP) continuously. Piping was constructed so that treated it was able to inject not feed water but treated water into the membrane module when performing B/W to realize automatic operation.

2.4. Operating conditions

This experiment was carried out automatically and continuously through the laptop, and the concentration of feed water was set at 5,000 mg/L suspended solids. The feed water tank temperature was maintained at $20^{\circ}\text{C} \pm 0.5^{\circ}\text{C}$ using a water bath to minimize the effect depending on temperature changes. Through the preliminary test, the stable operation was performed at $1 \text{ m}^3/\text{m}^2 \text{ h}$ as an air scrubbing condition for polymeric and ceramic membranes, and the experiments were conducted applying this. The polymeric membrane was operated at 5 and 10 LMH through the preliminary test, and the ceramic membrane was also operated at 150 and 280 LMH. Before performing membrane fouling, all the membranes were flushed using deionized water to carry out the experiments.

2.5. Measurement fouling mechanism

Concentrations increase around the membrane surface when membrane fouling is caused by pressure. The cake filtration theory is one of the theoretical equations representing this. The solvent permeate flux in the cake filtration theory can be expressed based on the following Darcy's law [11–13]:

$$R_c = \frac{\Delta P}{\mu(R_m + R_a + R_p + R_g + R_c)} \quad (1)$$

where μ is solvent viscosity coefficient; R_m is the resistance of membrane itself; R_a is resistance by adsorption; R_p is resistance by clogging in the membrane; R_g is resistance by gel deposits on membrane surface; R_c is resistance by deposition of cake layers; ΔP is net driving pressure in membrane filtration.

Assuming that membrane fouling occurs only in cake form, $R_a = R_p = R_g = 0$. Thus, it can be expressed as follows:

$$J = \frac{\Delta P}{\mu(R_m + R_c)} \quad (2)$$

When R_m is proportional to the mass of membrane foulants deposited on the membrane surface and operation is performed at the same pressure, R_c can be expressed as follows [14–16]:

$$R_c = \frac{\alpha C_b V}{A} \quad (3)$$

Table 1
Feed water properties

Parameters	Values
Sodium (mg/L)	40.751
Ammonium (mg/L)	58.370
Total chlorophyll (g/100 g)	20.7
Water content (%)	98.88
pH	7.5–7.9
SS (mg/L)	5,100

where α is specific cake resistance; C_b indicates the mass of dry cake solids per volume of filtrate; V is cumulative permeate quantity; A is an effective area of the membrane.

The fouling formation mechanisms of the polymeric and ceramic membranes were analyzed using the following methods: The fouling formation mechanisms were analyzed by applying the filtration resistance obtained by filtering feed water through the initial membrane, the filtration resistance obtained by repeating TMP and a constant cycle, and TMP to Hermia's model. It has been reported that Hermia's model is appropriate to explain the fouling mechanism using permeate flux in membrane filtration [17,18]. The calculation was conducted using the following four equations:

Complete blocking model:

$$\ln J_p = \ln J_0 - K_c t \quad (4)$$

where K_c membrane surface blocked per unit of the total volume that permeates through the membrane; J_0 initial permeate flux.

The above phenomena occur when the solute is larger than the membrane pore size.

Intermediate blocking model:

$$\frac{1}{J_p} = \frac{1}{J_0} + K_i t \quad (5)$$

where K_i is membrane surface blocked per unit of the total volume that permeates through the membrane

The intermediate blocking model occurs when the solute is similar in pore size.

Standard blocking model:

$$\frac{1}{J_p^{1/2}} = \frac{1}{J_0^{1/2}} + K_0 t \quad (6)$$

The standard blocking model occurs in the membrane by molecules smaller than the membrane pore size.

Cake layer formation model:

$$\frac{1}{J_p^2} = \frac{1}{J_0^2} + K_{gl} t \quad (7)$$

In this case, a cake layer is formed on the membrane surface. The solute does not penetrate into the membrane and then is precipitated on the membrane surface because it is larger than membrane pore size.

3. Results and discussion

3.1. Flux curves and resistance analyses

Fig. 2 shows the filtration resistance depending on polymeric membrane LMH. Fig. 3 shows the filtration resistance depending on ceramic membrane LMH. The polymeric and the ceramic membrane LMHs have experimented under the conditions selected by the preliminary test. According to a report, membrane fouling by algae is worsened by EPS and is very sensitive to flux, and it is important to find out the optimal productivity [19]. The results of this experiment also show that TMP increases with increasing LMH, and it is considered that algal matter caused membrane fouling. As shown in Figs. 2 and 3, the stable operation was realized at 5 and 150 LMH in the polymeric and ceramic membranes, respectively.

Fig. 4 shows the TMP of the results of the stably operated two different membranes. Fig. 4 shows the operating conditions used to analyze the membrane formation mechanisms using Hermia's model in the next paragraph. The more stable operation was performed even though the ceramic membrane shows high LMH.

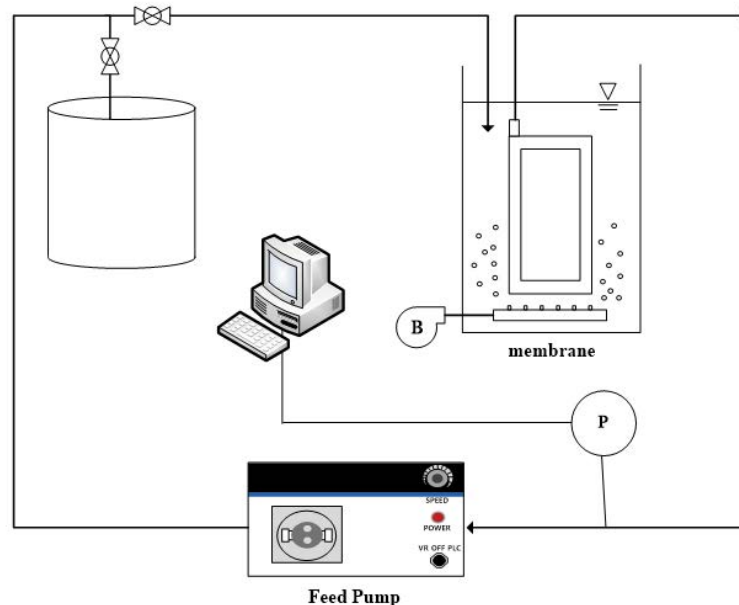


Fig. 1. Schematic diagram of the lab-scale continuous test unit.

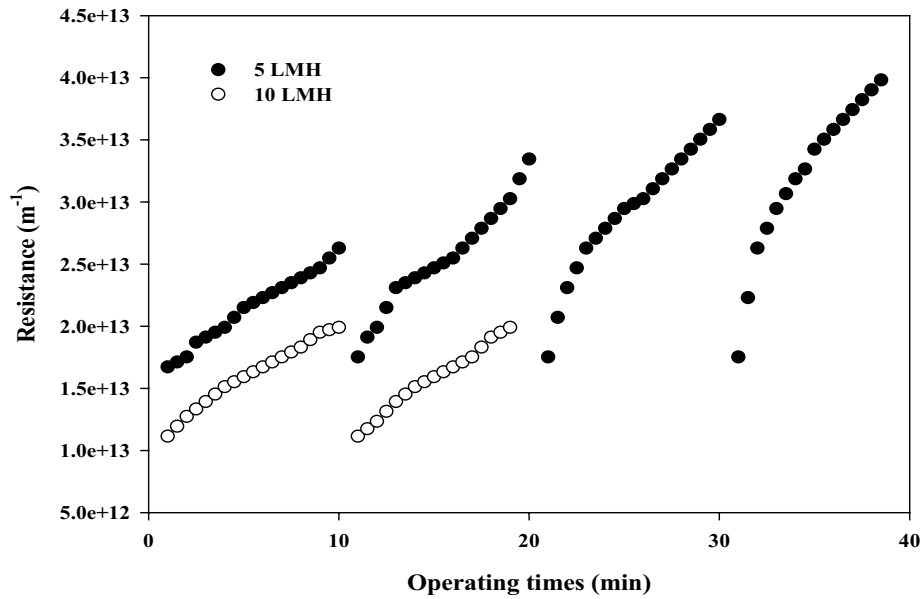


Fig. 2. Results of changes in filtration resistance according to polymeric membrane LMH.

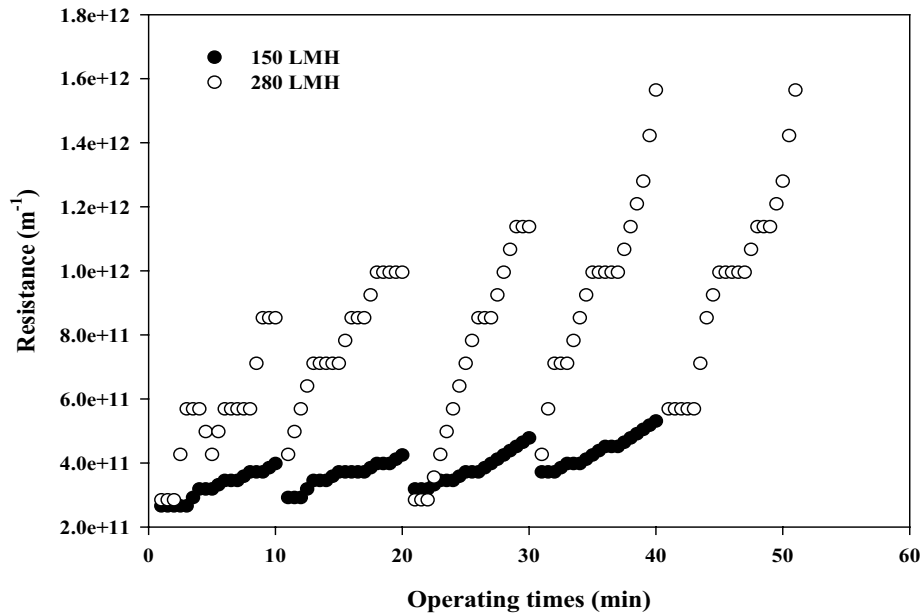


Fig. 3. Results of changes in filtration resistance according to ceramic membrane LMH.

Hofs et al. [20] reported that highly negative charge or hydrophilic membranes cause less fouling under the same conditions. The ceramic membrane shows stable operation also in this experiment. It is considered that ceramic membranes made of SIC are resistant to fouling because they are more hydrophilic than polymeric membranes made of PVDF.

3.2. Normalized flux measurement

To analyze the fouling formation mechanisms depending on the operating conditions of polymeric and ceramic membranes, Figs. 5a and b show the normalized flux. As

shown in the figures, flux decreases in every filtration cycle, and it means that fouling occurs on membranes. Recovery by B/W decreases as the experiments progress, and then fouling increases. The experiments were stopped in the section where the initial flux decreased by 40%–50%, and then it was considered that irreversible fouling was formed in *B* (*A*: the initial cycle, *B*: the cycle flux decreased). The polymeric membranes in Fig. 5a recover flux for each B/W cycle, but the ceramic membranes in Fig. 5b cannot recover to the initial flux with the passage of the filtration cycle and then show a tendency to be worsened gradually. Fig. 6 is a graph showing reversibility and irreversibility by

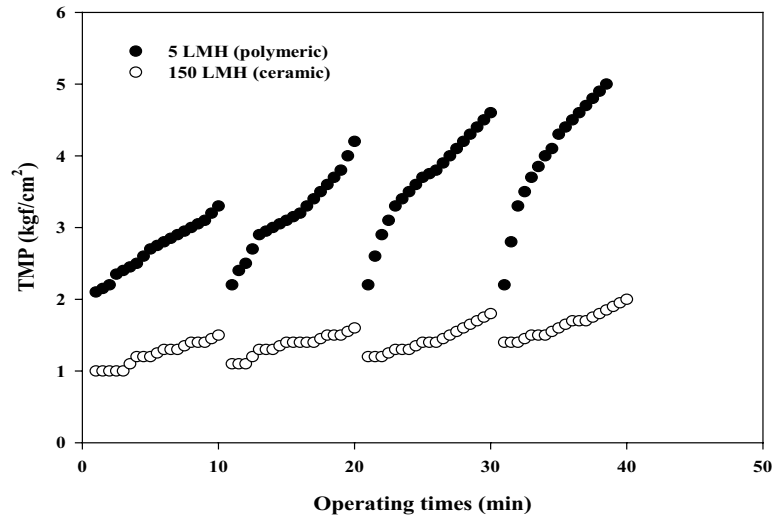


Fig. 4. Comparison of changes in TMP of polymeric and ceramic membranes.

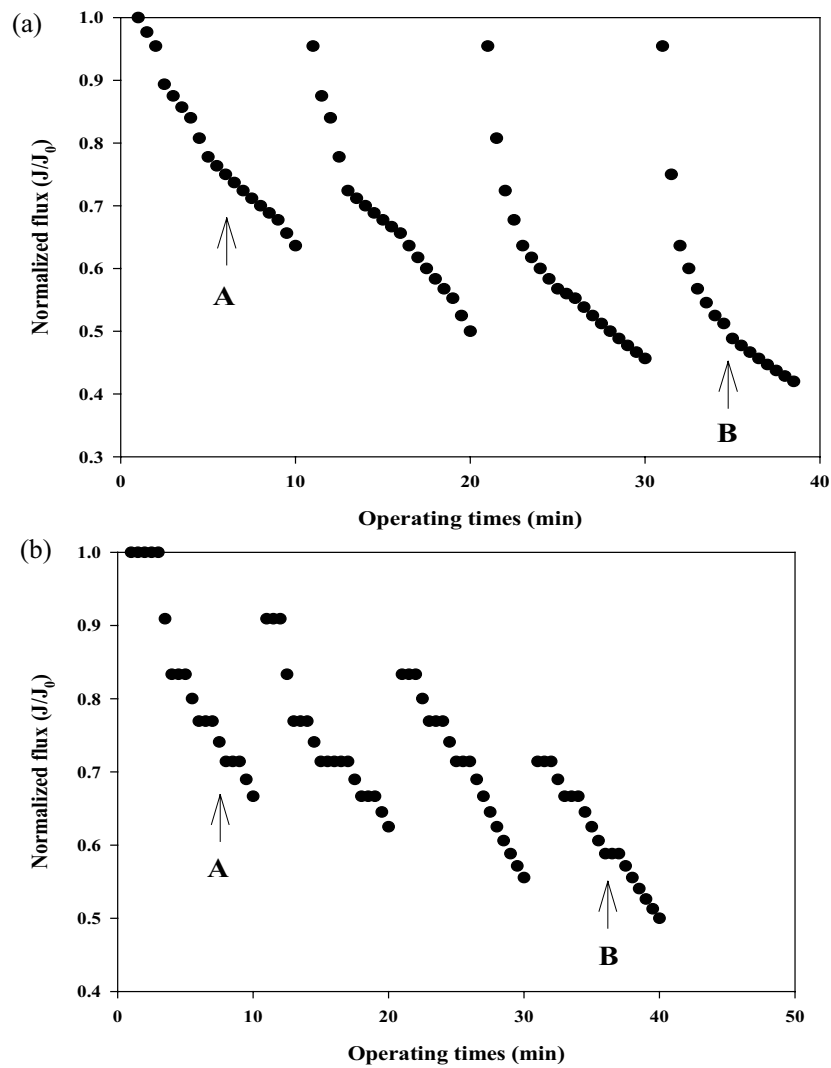


Fig. 5. Normalized fluxes of polymeric and ceramic membranes (a) Normalized flux of polymeric membranes and (b) Normalized flux of ceramic membranes.

membrane material with a fouling ratio. Wang et al. [21] reported that membrane fouling is worsened in the operation at higher flux. It is considered that fouling in the ceramic membranes was worsened also in this study because the

flux of ceramic membranes was much higher than that of polymeric membranes.

3.3. Analysis of membrane fouling formation mechanisms using Hermia's model

Figs. 7a–d are graphs applying the experimental results of the polymeric membranes to Hermia's model. R^2 values make it possible to analyze which model caused membrane fouling formation. In other words, R^2 values show a correlation with each model. First, Fig. 7a shows the complete pore blocking in the experiments for the polymeric membranes. Although 1 cycle shows a high correlation (R^2 value: 0.9811), the R^2 value dramatically decreases to 0.8318 in 4 cycles. Fig. 7b shows the standard pore blocking. The R^2 value shows a tendency to decrease from 0.9731 to 0.7821 with the passage of the filtration cycle. Fig. 7c shows the intermediate pre-blocking. The R^2 value decreases from 0.9915 to 0.9130 with the passage of the filtration cycle. Fig. 7d shows the cake filtration. The R^2 value decreases from 0.9939 to 0.9658. Thus, different correlations for each model are found even in the same membrane.

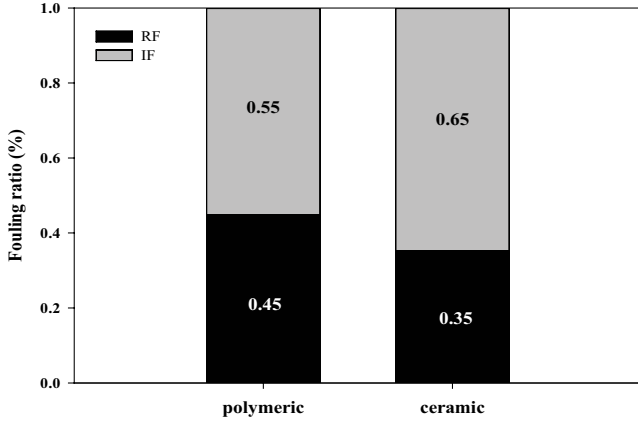


Fig. 6. Comparison of reversibility and irreversibility by material.

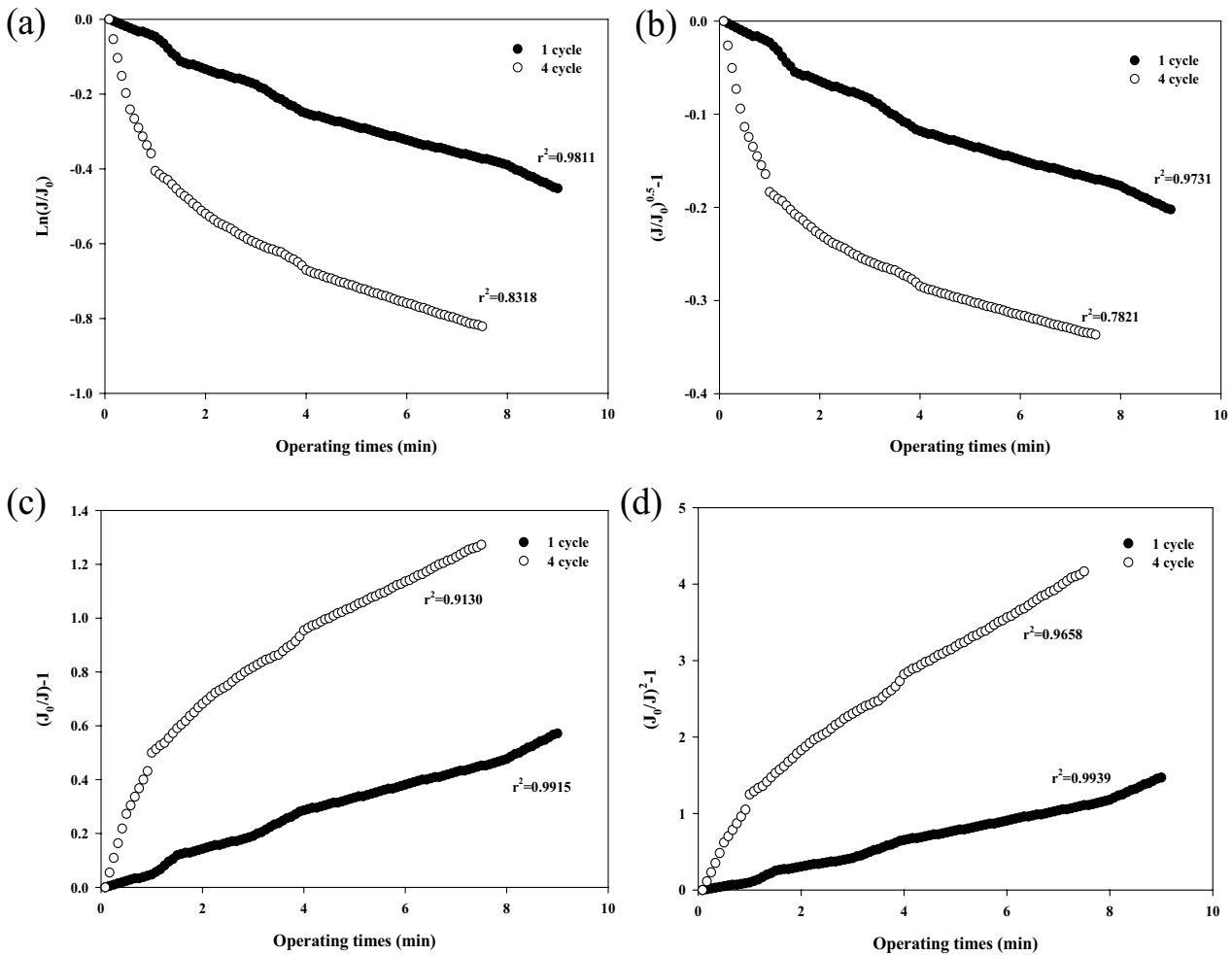


Fig. 7. Linear regression of normalized data (polymeric) (a) complete blocking, (b) standard pore blocking, (c) intermediate pore blocking, and (d) cake filtration.

Figs. 8a–d are graphs applying the experimental results of the ceramic membranes. First, each represents the complete pore blocking, standard pore blocking, intermediate pore blocking, and cake filtration. In Figs. 8a–d, the R^2 values changed from 0.9483 to 0.9844, from 0.9401 to 0.9865, from 0.9607 to 0.9764, and from 0.9671 to 0.9634, respectively. Fig. 9 is a graph applying the 4 cycle data for each blocking to Hermia's model to compare the fouling formation mechanisms by membrane material.

To determine the model close to the experimental data, the comparison was performed as shown in Table 3. Table 3 shows the R^2 value using a table to simplify the analysis of the graph data. First, concerning the polymeric membrane, the compatibility with all the models was high in 1 cycle, or the early filtration, but the effects of the complete pore blocking dramatically decreased with time, and then cake filtration became the major fouling mechanism. Also, it is considered that the standard pore-blocking does not affect fouling mechanisms. According to [22], particulate fouling in polymeric membrane filtration occurs mostly in the early filtration and then the blocking level decreases with time. The correlation

of the pore-blocking was high in the early filtration, but that of the cake filtration gradually increased also in this study. As for the ceramic membranes, the cake filtration showed high compatibility in the early filtration. However, the complete pore blocking and standard pore blocking gradually became the main fouling mechanisms. Karasuet al. [23] reported that ceramic membranes are hydrophilic and have lower protein fouling adhesion than relatively hydrophobic PVDF membranes. Lee et al. [24] reported that strong hydrophilicity of ceramic membranes has a relatively weaker correlation to foulants causing fouling compared to polymeric membranes. Hydrophilic membranes showed an extremely low tendency of fouling caused by algal substances, and membranes with hydrophobic surfaces showed a severe tendency of fouling due to algal filtration [25].

The fouling tendency of two membranes such as ceramic membranes made of silicon carbide representing hydrophobicity and polymeric membranes made of hydrophobic PVDF. It is considered that these tendencies occur by differences in membrane materials with hydrophilicity and hydrophobicity.

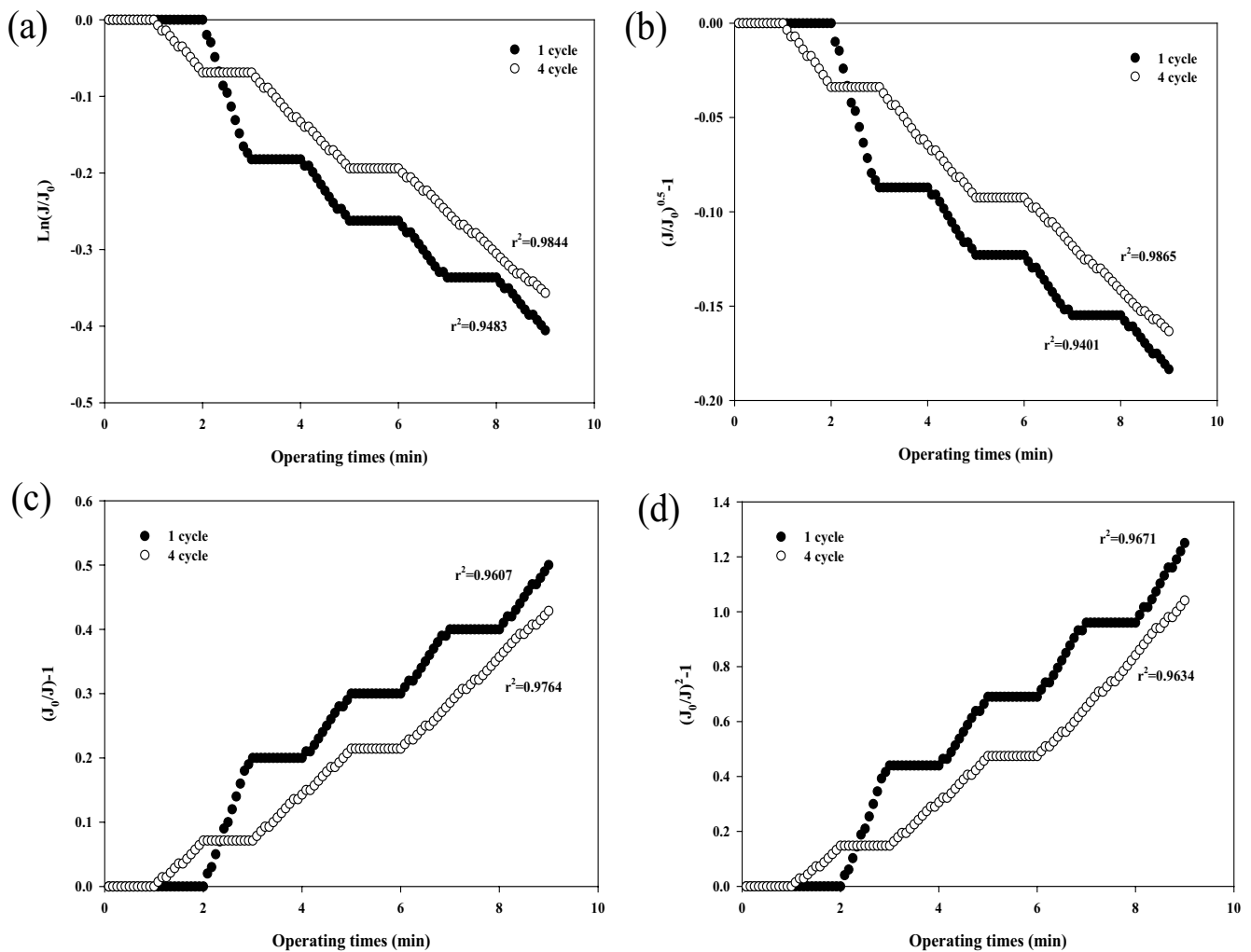


Fig. 8. Linear regression of normalized data (ceramic) (a) complete blocking, (b) standard pore blocking, (c) intermediate pore blocking, and (d) cake filtration.

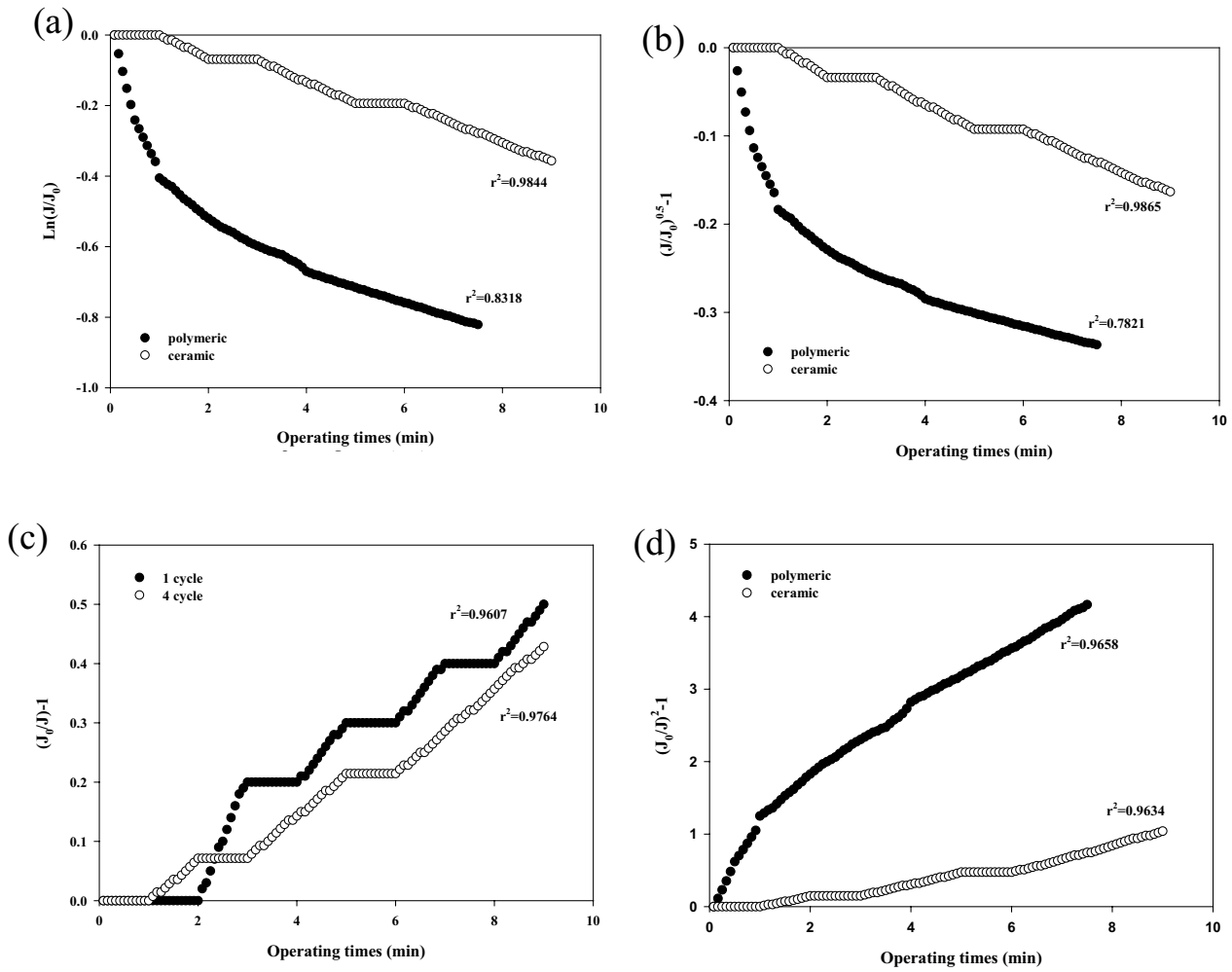


Fig. 9. Comparison of normalized data (polymeric and ceramic) (a) complete blocking, (b) standard pore blocking, (c) intermediate pore blocking, and (d) cake filtration.

Table 2
Specifications of membranes

	Membrane material	Effective membrane area (m ²)	Membrane type	Pores if the MF membrane (μm)	Clean water permeability (LMH/bar)
Ceramic	Silicon carbide	0.00652	Flat type	0.1	5,000
polymeric	PVDF	0.055	Hollow fiber	0.1	>500

Table 3
R² values of Hermia’s models

	Complete pore blocking	Standard pore blocking	Intermediate pore blocking	Cake filtration
Polymeric (1 cycle)	0.9811	0.9731	0.9915	0.9939
Polymeric (4 cycle)	0.8318	0.7821	0.9130	0.9658
Ceramic (1 cycle)	0.9483	0.9401	0.9607	0.9671
Ceramic (4 cycle)	0.9844	0.9865	0.9764	0.9634

4. Conclusions

This paper aimed to analyze the membrane fouling formation mechanisms in membrane processes applied from the perspective of algae harvesting. This paper also compared the membrane fouling mechanisms depending on operating conditions and membrane materials using high concentrations of artificial algae and Hermia's model. The following conclusions were drawn:

- When filtering polymeric and ceramic membranes in high concentrations of artificial algae raw water, it was able to operate ceramic membranes with much higher LMH. It was confirmed that fouling occurs less frequently due to ceramic membranes' properties such as hydrophilicity and highly negative charge.
- Hermia's model was used to examine the membrane fouling mechanisms. As a result, the polymeric membrane was in proximity to all the four models including the complete pore blocking, but the polymeric membrane was suitable for the cake filtration model with the passage of filtration.
- Although the ceramic membranes were highly correlated with the cake filtration model in the early filtration, the complete pore blocking and standard pore blocking models showed a tendency to be major fouling mechanisms with time.
- Both results showed different fouling formation mechanisms. It is considered that this was caused by the hydrophilicity of the polymeric membranes and the relative hydrophobicity of the ceramic membranes. It was confirmed that the fouling tendency varied from membrane materials. Membrane materials are regarded as a major reason.

Based on the results, examining the fouling formation mechanisms using Hermia's model is considered as an important factor in fouling control when applying membrane processes from the perspective of algae harvesting. It is considered necessary to examine fouling properties in more detail by analyzing fouling layers attached to the membrane surface with the progression of filtration in future research.

Acknowledgments

This work was supported by the Korea Environment Industry & Technology Institute (KEITI) through the Public Technology Program based on the Environmental Policy Project, funded by the Korea Ministry of Environment (MOE) (grant number 2018000200005).

References

- [1] S. Babel, S. Takizawa, H. Ozaki, Factors affecting seasonal variation of membrane filtration resistance caused by *Chlorella* algae, *Water Res.*, 36 (2002) 1193–1202.
- [2] X.Z. Zhang, Q. Hu, M. Sommerfeld, E. Puruhito, Y.S. Chen, Harvesting algal biomass for biofuels using ultrafiltration membranes, *Bioresour. Technol.*, 101 (2010) 5297–5304.
- [3] M. Rickman, J. Pellegrino, R. Davis, Fouling phenomena during membrane filtration of microalgae, *J. Membr. Sci.*, 423 (2012) 33–42.
- [4] Y.-T. Chiou, M.-L. Hsieh, H.-H. Yeh, Effect of algal extracellular polymer substances on UF membrane fouling, *Desalination*, 250 (2010) 648–652.
- [5] N.H. Lee, G. Amy, J.-P. Croué, H. Buisson, Identification and understanding of fouling in low-pressure membrane (MF/UF) filtration by natural organic matter (NOM), *Water Res.*, 38 (2004) 4511–4523.
- [6] G. Zhang, B. Wang, P. Zhang, L. Wang, H. Wang, Removal of algae by sonication-coagulation, *J. Environ. Sci. Health., Part A*, 41 (2006) 1379–1390.
- [7] J.-J. Chen, H.-H. Yeh, I.-C. Tseng, Effect of ozone and permanganate on algae coagulation removal – pilot and bench scale tests, *Chemosphere*, 74 (2009) 840–846.
- [8] Y.W. Liu, X. Li, Y.L. Yang, S. Liang, Fouling control of PAC/UF process for treating algal-rich water, *Desalination*, 355 (2015) 75–82.
- [9] L. Heng, Y. Yanling, G. Weijia, L. Xing, L. Guibai, Effect of pretreatment by permanganate/chlorine on algae fouling control for ultrafiltration (UF) membrane system, *Desalination*, 222 (2008) 74–80.
- [10] X. Zhang, L. Fan, F.A. Roddick, Understanding the fouling of a ceramic microfiltration membrane caused by algal organic matter released from *Microcystis aeruginosa*, *J. Membr. Sci.*, 447 (2013) 362–368.
- [11] S. Whitaker, Flow in porous media I: a theoretical derivation of Darcy's law, *Transp. Porous Media*, 1 (1986) 3–25.
- [12] K. Damak, A. Ayadi, B. Zeghmami, P. Schmitz, A new Navier-Stokes and Darcy's law combined model for fluid flow in crossflow filtration tubular membranes, *Desalination*, 161 (2004) 67–77.
- [13] L. Huang, M.T. Morrissey, Fouling of membranes during microfiltration of surimi wash water: roles of pore blocking and surface cake formation, *J. Membr. Sci.*, 144 (1998) 113–123.
- [14] W. Yuan, A. Kocic, A.L. Zydney, Analysis of humic acid fouling during microfiltration using a pore blockage–cake filtration model, *J. Membr. Sci.*, 198 (2002) 51–62.
- [15] S. Mattaraj, C. Jarusutthirak, R. Jiratananon, A combined osmotic pressure and cake filtration model for crossflow nanofiltration of natural organic matter, *J. Membr. Sci.*, 322 (2008) 475–483.
- [16] C. Duclos-Orselo, W. Li, C.-C. Ho, A three mechanism model to describe fouling of microfiltration membranes, *J. Membr. Sci.*, 280 (2006) 856–866.
- [17] M.C.V. Vela, S.A. Blanco, J.L. García, E.B. Rodríguez, Analysis of membrane pore blocking models applied to the ultrafiltration of PEG, *Sep. Purif. Technol.*, 62 (2008) 489–498.
- [18] A. Salahi, M. Abbasi, T. Mohammadi, Permeate flux decline during UF of oily wastewater: experimental and modeling, *Desalination*, 251 (2010) 153–160.
- [19] F. Wicaksana, A.G. Fane, P. Pongpairaj, R. Field, Microfiltration of algae (*Chlorella sorokiniana*): critical flux, fouling and transmission, *J. Membr. Sci.*, 387 (2012) 83–92.
- [20] B. Hof, J. Ogier, D. Vries, E.F. Beerendonk, E.R. Cornelissen, Comparison of ceramic and polymeric membrane permeability and fouling using surface water, *Sep. Purif. Technol.*, 79 (2011) 365–374.
- [21] Z. Wang, Z. Wu, G. Yu, J. Liu, Z. Zhou, Relationship between sludge characteristics and membrane flux determination in submerged membrane bioreactors, *J. Membr. Sci.*, 284 (2006) 87–94.
- [22] K.-J. Hwang, C.-Y. Liao, K.-L. Tung, Analysis of particle fouling during microfiltration by use of blocking models, *J. Membr. Sci.*, 287 (2007) 287–293.
- [23] K. Karasu, N. Glennon, N.D. Lawrence, G.W. Stevens, A.J. O'Connor, A.R. Barber, S. Yoshikawa, S.E. Kentish, A comparison between ceramic and polymeric membrane systems for casein concentrate manufacture, *Int. J. Dairy Technol.*, 63 (2010) 284–289.
- [24] S.-J. Lee, M. Dilaver, P.-K. Park, J.-H. Kim, Comparative analysis of fouling characteristics of ceramic and polymeric microfiltration membranes using filtration models, *J. Membr. Sci.*, 432 (2013) 97–105.
- [25] X. Sun, C. Wang, Y. Tong, W. Wang, J. Wei, A comparative study of microfiltration and ultrafiltration for algae harvesting, *Algal Res.*, 2 (2013) 437–444.